ACS Photonics

Letter

pubs.acs.org/journal/apchd5

Optical Rotation Reversal in the Optical Response of Chiral Plasmonic Nanosystems: The Role of Plasmon Hybridization

Mario Hentschel,[†] Vivian E. Ferry,[‡] and A. Paul Alivisatos*[,†,§,∥,⊥]

[†]Materials Science Division, Lawrence Berkeley National Laboratory, 1 Cyclotron Road, Berkeley, California 94720, United States

[‡]Department of Chemical Engineering and Materials Science, University of Minnesota−Twin Cities, 421 Washington Avenue SE, Minneapolis, Minnesota 55455, United States

[§]Department of Chemistry, [∥]Department of Materials Science, and [⊥]Kavli Energy NanoScience Institute, University of California−Berkeley, Berkeley, California 94720, United States

ABSTRACT: Chirality is an important molecular property for structural analysis. Similarly, it has been shown that plasmonic chiral systems exhibit strong circular dichroism (CD) responses that can be used to determine the relative positions of their constituent plasmonic elements. Here we show that the sign of the circular dichroism spectrum in a plasmonic system can be controllably changed through small geometric perturbations that change the energetic ordering of the hybridized modes. This mechanism is distinct from geometrical changes that explicitly change the handedness of the system. In a simple system composed of two stacked L-shaped resonators we observe a reversal of the optical rotation spectral signature for small relative shifts, and we show through electromagnetic modeling and experiments on lithographically patterned samples that this is due to a rearrangement of the relative energies between modes. The plasmonic system allows for geometric perturbation along controlled directions and therefore offers more control than corresponding molecular examples. Interestingly, this strong sensitivity in the optical response encodes more spatial information into the optical spectrum, emphasizing the importance of chiral plasmonic assemblies for structural investigations on the nanoscale.

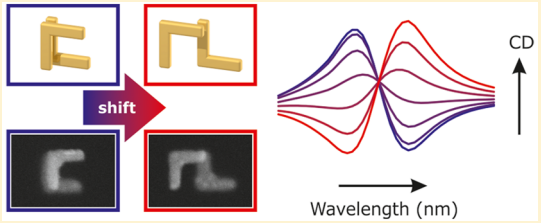

KEYWORDS: *surface plasmons, circular dichrosim, chirality, plasmon hybridization*

Circular dichroism (CD) spectroscopy is frequently used to characterize chiral molecules by measuring the differential absorption of right- and left-handed circularly polarized light, and has been used as a structural probe for a variety of systems including charge transfer in inorganic complexes and conformational changes in biomolecules.[1−3] However, the relationship between the absolute configuration of a molecule and the sign of the CD spectrum is complex. Indeed while the sign of the CD spectrum is reversed for true enantiomers, it is often not possible to correlate the configuration of related molecules and the sign of their resulting CD spectra without more complex analysis. In chiral chelated compounds derived from octahedral metal−ligand complexes, for example, the d-orbitals are closely spaced in energy and each transition differentially absorbs the two circular polarizations of light.[4,5] A small perturbation in the ligands may change the ordering of these energy levels without changing the symmetry of each level. Therefore, when comparing two related compounds with reversed energy level ordering, the sign of the CD spectrum could reverse at a given energy due to the changing character of the excitation. Here we demonstrate an analogous plasmonic chiral assembly where a change in optical rotation is observed due to systematic tuning of the hybridized mode energies.

The past few years have seen a steady increase in interest in plasmonic analogues of chiral molecules. A number of interesting systems have been demonstrated, ranging from two-dimensional chiral systems,[6−11] to solid metallic nanospirals[12−18] and handed individual nanoparticles,[19−21] to complex chiral arrangements of achiral metallic nanoparticles.[22−31] The observed phenomena in plasmonic systems are orders of magnitude stronger than in the corresponding molecular systems due to the large interaction strength of plasmonic resonances with the external light field. The strength of the interaction is sufficient to allow for the development of thin absorptive or reflective quarter-wave plates and similar systems.[12,24,32,33] Apart from these fundamental studies, researchers have used plasmonic materials as chirality sensors[34,35] or observed other intriguing phenomena, e.g., nonlinear optical activity.[36] Chiral plasmonic systems have also been proposed as three-dimensional plasmon rulers for their ability to encode structural information in the CD spectrum.[37−40]

In this paper, we show that the sign of the CD spectrum in a plasmonic assembly may be controlled by tuning the relative energies of the hybridized modes, similarly to the molecular example described above. The system consists of two stacked L-shaped plasmonic nanostructures and is designed such that right-handed circularly polarized light (RCP) and left-handed circularly polarized light (LCP) each preferentially excite one hybridized mode in the plasmonic assembly. The two modes have distinct resonant energies. As the geometry is continuously

Received: June 26, 2015
Published: August 12, 2015

DOI: 10.1021/acsphotonics.5b00354
ACS Photonics 2015, 2, 1253−1259

tuned through small lateral changes, the spectral position of these modes relative to one another shifts, eventually causing a change in the sign of the pseudoscalar CD function at a given energy. Importantly this is a distinct mechanism from tunable chiral systems where the handedness clearly reverses under geometric modification.[15] The key difference between this system and a molecular system is the ease of tuning the relative energies: here the relative energies of the RCP and LCP modes are actively changed through a controllable lateral displacement. The tunability of the optical properties of plasmonic assemblies is one of their key attributes.[41,42] In a plasmonic oligomer these changes could therefore be accessed in a single dynamic system, which could find application as switchable metamaterials or as a nanoscale structural sensor.

Figure 1a depicts a sketch of the investigated geometry. Our structure consists of two stacked and rotated L-shapes. The

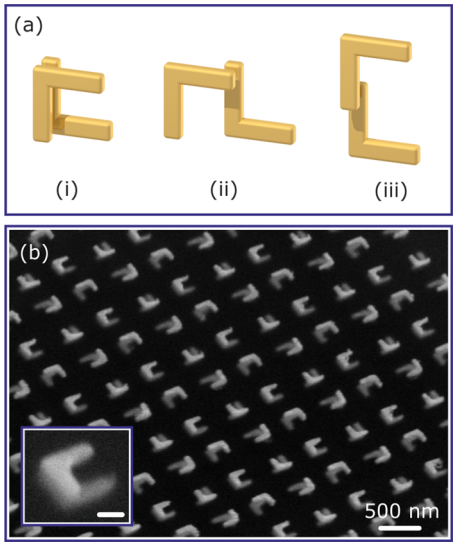

Figure 1. (a) Sketch of the investigated chiral plasmonic system. The structure consists of two stacked L-shapes. The design allows for the lateral displacement of the upper layer L-shape with respect to the lower one. (b) Tilted SEM overview and close-up images of the fabricated sample, here with zero lateral displacement. The individual dimers are arranged in a C_4-symmetric lattice in order to avoid polarization conversion. The geometrical dimensions (in simulation and experiment) are L-shape arm length 200 nm, width 70 nm, thickness 40 nm, and surface-to-surface distance between the L-shapes 80 nm. Scale bars are 500 nm for the overview and 100 nm for the close-up.

assembly is characterized by the size of the individual L-shapes, their out-of-plane spacing, and a lateral shift (horizontally or vertically). We will investigate in simulation and experiment the optical response of the system under lateral shifts of the upper layer L-shape with respect to the lower layer one, as indicated in Figure 1a. Figure 1b depicts a tilted-view SEM overview and close-up image of the fabricated two-layer structure with zero lateral displacement. In the experiment the structures are realized in a C_4-symmetric lattice in order to avoid contributions of polarization conversion to the observed CD signal.[43]

Figure 2a shows simulated extinction cross section spectra for left- and right-hand circularly polarized light incident on a single two-L-shape system with no lateral displacement between the layers (for simulation details refer to the Methods section). One resonance is observed each for LCP and RCP excitation. The out-of-plane spacing distance of 80 nm between

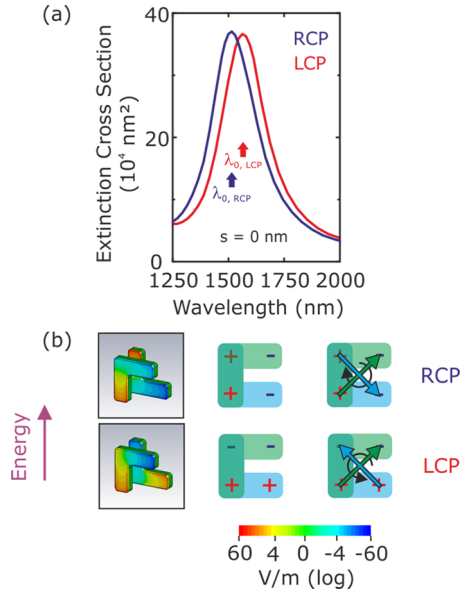

Figure 2. Simulated extinction cross sections and field distributions for two stacked L-shapes with an out-of-plane spacing of 80 nm and no lateral displacement. (a) The extinction cross section spectra for RCP and LCP excitation show one resonance each as the bonding and antibonding combination of the individual modes of the L-shapes. The modes have a distinct rotational character and are, thus, given the correct vertical spacing, excited by one polarization state each with extremely high preference. (b) Field distributions at the spectral position as indicated by the red and blue arrows in (a) (1514 and 1560 nm, respectively). From the simplified sketch it is apparent that the lower energy mode has a clear left-handed character; the higher energy one, a clear right-handed one.

the two layers has been optimized such that the two hybrid modes in the combined system are each highly preferentially excited by LCP and RCP light.[44] Figure 2b depicts the calculated electric field distributions (normal component) for RCP and LCP excitation at the spectral positions indicated by the blue and red arrows in (a). As can be seen from the simplified sketch of the two modes, the lower energy symmetric combination of the two individual L-shape modes has a left-handed character. The higher energy antisymmetric combination has clear right-handed character. Due to the optimized vertical distance between the two layers, the left- and right-handed modes will be mainly excited by the respective light field. Only the polarization state with the correct handedness matches the rotational sense of the induced electric dipole moments (sketched on the rightmost side) as well as their pitch (that is, the rotation of the incident electric field vector per unit length).[44] Note that for an unoptimized out-of-plane spacing both modes can be efficiently excited by both polarizations, so the relative excitation strengths will be different. In these cases, the spectra for RCP and LCP excitation will exhibit two resonances each. As the out-of-plane spacing thickness has a fixed value, the ideal optimized situation is no longer fulfilled as soon as the hybrid modes spectrally shift. However, the change in wavelength and therefore pitch of the incoming exciting handed light field is minute. Thus, it also causes only a minute cross excitation. Such a small cross excitation will lead to a nearly negligible spectral broadening of the two observed plasmonic modes. For increasing mismatch of the out-of-plane spacing thickness with the ideal one, first a shoulder and a subsequent second peak will form.

DOI: 10.1021/acsphotonics.5b00354
ACS Photonics 2015, 2, 1253−1259

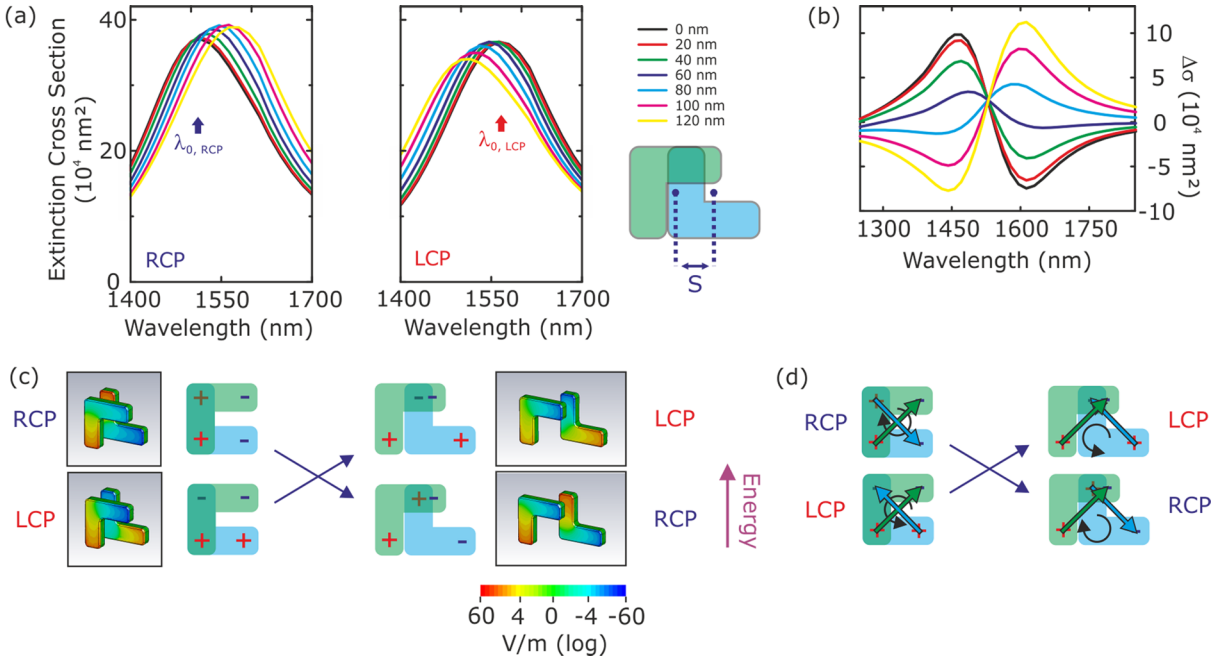

Figure 3. Simulated extinction cross sections and electric field distribution for a horizontal displacement s between the two L-shapes. (a) Extinction cross sections for RCP and LCP excitation. The mode excited by RCP light undergoes a continuous red-shift; the one excited by LCP light, a continuous blue-shift. (b) Calculated CD spectra. The absolute value of the CD diminished, the spectral signature inverts, and subsequently the CD increases again. (c and d) Simulated electric field distributions and mode sketches. The lateral displacement leads to an inversion of the plasmon hybridization scheme, while the modes retain their rotational sense, explaining the apparent change in handedness as indicated by the CD spectra in (b). Spectral position of the simulated field distributions: 1514 and 1560 nm (s = 0 nm) and 1514 and 1578 nm (s = 120 nm).

Next we investigate the influence of the lateral displacement between the two individual layers. Figure 3a depicts the simulated extinction cross sections for a horizontal shift s between the two layers. The hybridized plasmonic mode excited by RCP light undergoes a continuous red-shift for increasing displacement s. Simultaneously, the mode excited by LCP light undergoes a continuous blue-shift. Closely examining the spectra reveals that the energetic splitting between the two excited modes decreases and reaches zero for a horizontal displacement between 60 and 80 nm and subsequently increases again. The two modes therefore cross in resonance energy and exchange their relative spectral position. The reason for the spectral shift lays in the changed interaction strength between the individual dipolar plasmonic modes of the L-shape. As sketched in Figure 3c, the overlap between the plasmonic modes changes. This causes a change in the interaction strength between the two modes and thus changes the energetic splitting between the newly formed hybrid modes. However, the change in interaction strength is not a continuous function of the displacement. First the interaction strength diminishes until a shift of $s \approx 60$ nm and then increases again, matching the observed crossing in the spectral position.

Figure 3b depicts the CD spectra of the stacked system, defined as the difference of the extinction cross sections for RCP and LCP excitation. As expected by energy conservation, the CD spectrum vanishes nearly completely when integrated with respect to energy. The CD spectra show a monotonic decrease in absolute value followed by an inversion of the sign and subsequent monotonic increase in the absolute CD value. The simulated electric field distributions (normal component) shown in Figure 3c explain the observed behavior: a horizontal shift between the two layers leads to an inversion of the plasmon hybridization scheme. The electric field distributions are shown for the two extremes considered here, although it is important to note that the inversion of the CD sign occurs between s = 60 nm and s = 80 nm, not simply at any lateral shift away from s = 0. The energetically favorable symmetric combination of the two individual L-shapes for s = 0 nm becomes the energetically less favorable combination for s = 120 nm. Similarly, the energetically less favorable antisymmetric combination of the two individual L-shapes for s = 0 nm becomes the energetically favorable combination for s = 120 nm. Figure 3d depicts a simplified sketch of the field distribution and indicates the electric dipole moments of the individual layers. The character of the individual RCP and LCP modes has not changed under horizontal lateral displacement, but the relative energies of the RCP and LCP mode have exchanged. Thus, at a given energy, the CD spectrum may change sign with lateral displacement due to a change in the nature of the mode at that energy. This is distinct from a change in CD sign due to an explicit change in handedness.

Figure 4 depicts the simulated results for a vertical shift s' between the two L-shapes. The energetically higher mode excited by RCP light at s' = 0 nm continuously blue shifts with increasing vertical shift s', cf. Figure 4a. The energetically lower mode excited by LCP light at s' = 0 nm on the other hand continuously red-shifts. As a consequence, and in contrast to the horizontal shift, the energetic splitting between the two modes increases monotonically. Similarly to the horizontal case, the vertical displacement leads to a monotonic increase in the interaction strength between the two dipolar plasmonic modes of the L-shapes, which reaches its maximum around $s' \approx 120$ nm. Therefore, as expected, the CD spectra depicted in Figure 4b do not change their spectral signature. Instead we observe an increase in the spectral separation between the minimal and maximal CD values and a monotonic increase in the absolute CD value. The field distributions and mode sketches shown

DOI: 10.1021/acsphotonics.5b00354
ACS Photonics 2015, 2, 1253−1259

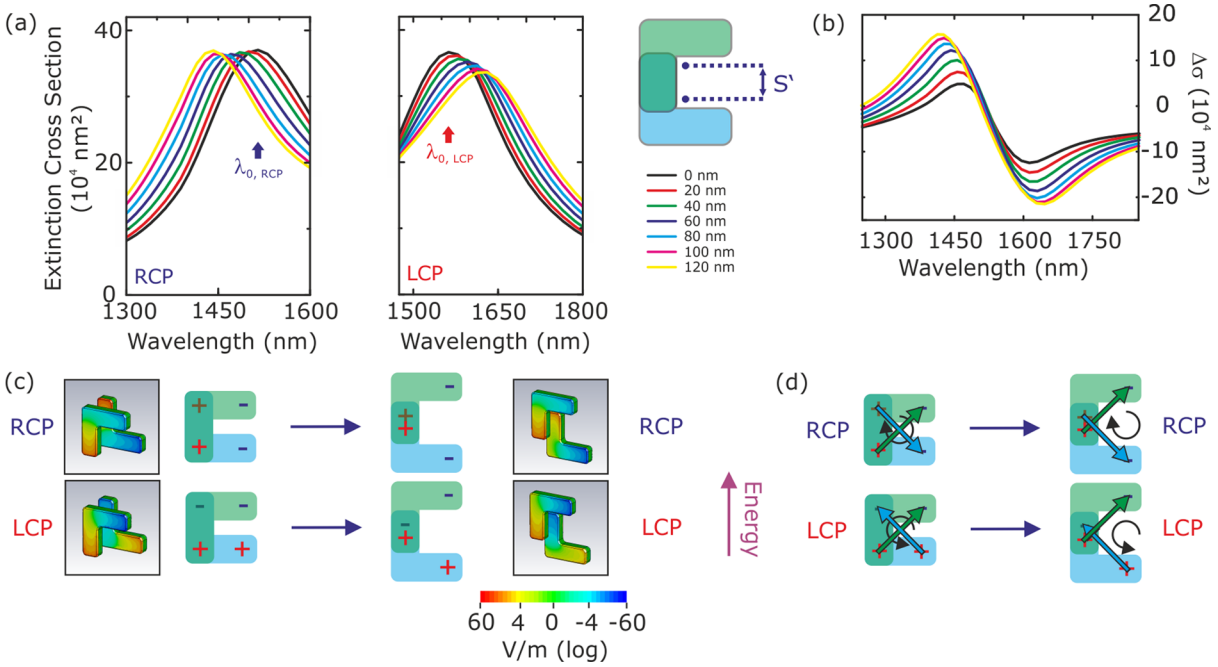

Figure 4. Simulated extinction cross sections and electric field distributions for a vertical displacement s' between the two L-shapes. (a) Extinction cross sections for RCP and LCP excitation. The mode excited by RCP light undergoes a continuous blue-shift, and the one excited by LCP light, a continuous red-shift, further increasing the energetic splitting between the modes. (b) Calculated CD spectra. The absolute value of the CD increases monotonically, and the spectral splitting between the minimum and maximum CD value increases. (c and d) Simulated electric field distributions and mode sketches. The vertical displacement increases the interaction strength between the elements and therefore the energetic splitting of the modes. The lower and higher energy modes remain the lower and higher energy modes and keep their respective sense of rotation. Positions of the simulated field distributions: 1514 and 1560 nm (s = 0 nm) and 1441 and 1621 nm (s = 120 nm).

in Figure 4c and d underline the observed phenomenon. The energetically favorable symmetric combination of the two individual L-shapes for s' = 0 nm remains the energetically favorable combination for s' = 120 nm, which also holds true for the energetically less favorable combination. Similarly to the case of a horizontal displacement, these two combinations also retain their sense of rotation as well as their respective exiting polarization state. Intuitively, one would expect that zero displacement leads to the highest interaction strength, which should therefore diminish with increasing displacement s' between the two L-shapes. Instead, increased interaction strength is observed as manifested by the increased splitting between the lower and higher energy mode. Inspecting the field distributions, it becomes obvious that larger displacements s' result in an improved spatial overlap of the plasmonic modes in the two L-shapes. However, it is important to note that this trend does not continue and the interaction strength will in fact decrease again for even larger displacements s' and approach zero for very large shifts. Examining the CD spectra in Figure 4b closely, one can already observe an onset of saturation of the maximum CD value, indicating that the maximum interaction strength has nearly been reached.

So far we have examined the optical response of the stacked L-shape system for two special cases, horizontal and vertical shifts. For all positions in between these two one might expect an additive behavior for the inversion and noninversion of the CD response. However, this is not what happens. In fact, these combined displacements map the interaction strength between the two L-shaped elements within the two-dimensional plane. Figure 5 depicts simulated results for this interaction strength, which manifests itself in the splitting of the antisymmetric and symmetric modes. This splitting is also found in the spectral separation between the minimum and maximum value of the CD spectra. Figure 5 shows a color map of the difference between the spectral position of the maximum extinction for LCP light and the maximum extinction for RCP light. The inversion of the spectral signature of the CD response therefore corresponds to a sign change in this difference for different relative displacements. The cases examined so far correspond to the horizontal line at s' = 0 nm and the vertical line at s = 0 nm. The color map is symmetric around the s = 0 nm line, which indicates that a horizontal shift leads to the same coupling effects for positive and negative shifts. Figure 5b illustrates that this is indeed correct, arguing from a geometrical standpoint. The two sketches are for s = 120 nm and s = −120 nm. Rotating the s = −120 nm case by 180° results in the same geometry as for s = 120 nm, except that the lower plane is the upper one and vice versa, which, however, does not make a difference for the optical response. For a shift in the vertical direction we observe a pronounced asymmetry. Again, from a geometrical standpoint the behavior is clear, as s' = 120 nm and s' = −120 nm lead to very different geometries, cf. sketches in Figure 5a. For increasing vertical displacement s' the zero crossing of the scattering maxima is shifted to higher and higher horizontal displacements s, which is expected from the already discussed interaction potential.

In order to verify our theoretical results we have fabricated a series of samples via standard two-layer electron beam lithography. Figure 6 depicts the measured 1-Transmittance spectra for RCP- and LCP-polarized incident light for a horizontal displacement of s = 0 nm and s = 150 nm in Figure 6a. For s = 0 nm the mode excited by LCP light is the lower energy one, whereas RCP light excites the higher energy mode. The spectrum for LCP excitation exhibits a small additional shoulder at higher energies. We conclude that in the experiment the out-of-plane spacing distance between the two layers is not optimal, and therefore there is a small

DOI: 10.1021/acsphotonics.5b00354
ACS Photonics 2015, 2, 1253−1259

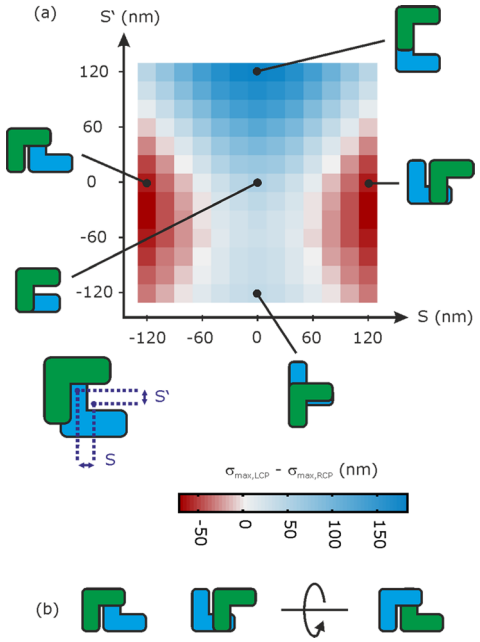

Figure 5. (a) Simulated "interaction" map. The color scale shows the difference between the spectral position of the maximum extinction for LCP light and the maximum extinction for RCP light. The inversion of the spectral signature of the CD response therefore corresponds to a sign change in this difference for different relative displacements. The step size in the simulation is 20 nm. (b) The map is symmetric around the S = 0 nm axis, as a shift s leads to the same geometry as $-s$.

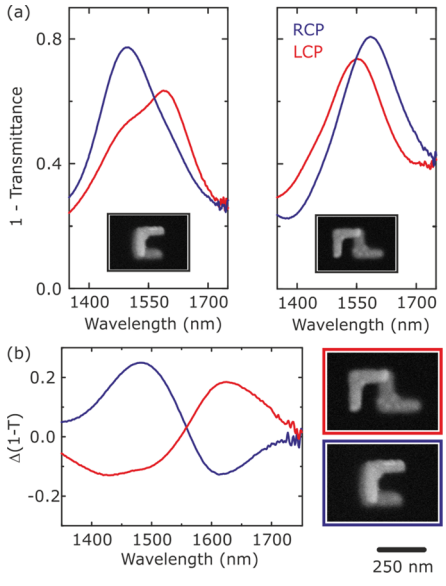

Figure 6. Experimental results for a horizontal shift between the two L-shapes of s = 0 nm and s = 150 nm. The fabricated geometrical parameters are arm length 200 nm, width 70 nm, thickness 40 nm, and surface-to-surface distance between the L-shapes 80 nm. (a) The modes excited by RCP- and LCP-polarized light exchange their energetic position and therefore lead to an inversion of the spectral signature in the CD spectra as shown in panel (b). The reason for the observed behavior is the inversion of the plasmon hybridization scheme as opposed to a clear change in geometric handedness.

"cross-excitation" between the modes. For s = 150 nm the excited modes have exchanged their energetic position, as predicted by the simulation. Figure 6b shows the CD spectra obtained from the experiment, which convincingly show the reversal in sign of the CD spectrum under horizontal displacement.

In conclusion, we have shown that the sign of the CD response in plasmonic assemblies may be reversed by manipulating the hybridized energies of the modes excited under RCP and LCP light. The symmetries of the modes excited under each polarization do not change, but their relative energetic ordering is reversed, leading to an inversion in the sign of the CD spectrum. In contrast to molecular examples, the plasmonic system exhibits greater control over the geometry and resulting spectrum, and this phenomenon can be accessed within a single plasmonic oligomer design through small lateral displacements. This phenomenon may find applications in switchable metamaterials or as a nanoscale structural sensor that encodes spatial position.

METHODS

Simulations. The simulated extinction cross section spectra and field distributions at the respective spectral positions were calculated using the software package CST Microwave Studio, Darmstadt, Germany. An experimentally measured dielectric function of gold was utilized in the simulations.[45] In the calculations, we embedded the plasmonic nanoparticles in a homogeneous medium with an effective refractive index n = 1.5 (refractive index of the dielectric spacer). In the experiment the C_4 symmetric lattice is required in order to render the grating superstructure uniaxial and therefore enable purely chiral eigenstates.[43] The interaction in the grating is a pure far-field effect and in general does not or only weakly influence(s) the plasmonic modes. We have thus decided to simulate a single cluster instead of the more complex C_4-symmetric grating.

Fabrication. First a glass substrate is coated with a 120 nm thick dielectric layer by spin-coating (IC1-200, Futurrex). The gold structures are defined by electron beam lithography (Crestec CABL-9510CC) in a positive resist (PMMA, Microchem) followed by thermal evaporation of a 3 nm Ti adhesion layer and 40 nm gold followed by a lift-off procedure. Subsequently, the sample is coated with another 120 nm thick dielectric layer. In order to promote adhesion of the dielectric layer, we utilized an adhesion promoter (SurPass 3000, DisChem). The second layer is exposed in an aligned second electron beam lithography step, followed by evaporation, lift-off, and a final planarization step. The footprint of each array is 30 × 30 μm^2.

Measurement. The optical response was evaluated using a Fourier-transform infrared spectrometer, combined with an infrared microscope giving extinction (1-Transmittance) spectra. The polarization was set with an infrared polarizer and a broadband quarter-wave plate (Thorlabs).

AUTHOR INFORMATION

Corresponding Author

*E-mail: alivis@berkeley.edu.

Notes

The authors declare no competing financial interest.

ACKNOWLEDGMENTS

M.H. gratefully acknowledges financial support by the Alexander von Humboldt Foundation through a Feodor Lynen Research Fellowship. This material is based upon work supported by the National Science Foundation under Grant DMR-1344290. The authors acknowledge the Marvell Nanofabrication Laboratory for

DOI: 10.1021/acsphotonics.5b00354
ACS Photonics 2015, 2, 1253−1259

the use of their facilities and the group of Xiang Zhang for the use of their FTIR spectrometer.

REFERENCES

(1) Barron, L. D. *Molecular Light Scattering and Optical Activity*, 2nd ed.; Cambridge Univ. Press, 2004.
(2) Berova, N.; Nakanishi, K.; Woody, R. W. *Circular Dichroism, Principles and Applications*; Wiley: New York, 2000.
(3) Luisi, P. L. *The Emergence of Life - From Chemical Origins to Synthetic Biology*; Cambridge University Press, 2006.
(4) Bosnich, B. The Application of Exciton Theory to the Determination of Teh Absolute Configuration of Inorganic Complexes. *Acc. Chem. Res.* **1969**, *2*, 266−273.
(5) Rodger, A.; Norden, B. *Circular Dichroism and Linear Dichroism*; Oxford University Press, 1997.
(6) Papakostas, A.; Potts, A.; Bagnall, D.; Prosvirnin, S.; Coles, H.; Zheludev, N. Optical Manifestations of Planar Chirality. *Phys. Rev. Lett.* **2003**, *90*, 107404.
(7) Canfield, B. K.; Kujala, S.; Kauranen, M.; Jefimovs, K.; Vallius, T.; Turunen, J. Remarkable Polarization Sensitivity of Gold Nanoparticle Arrays. *Appl. Phys. Lett.* **2005**, *86*, 183109.
(8) Kuwata-Gonokami, M.; Saito, N.; Ino, Y.; Kauranen, M.; Jefimovs, K.; Vallius, T.; Turunen, J.; Svirko, Y. Giant Optical Activity in Quasi-Two-Dimensional Planar Nanostructures. *Phys. Rev. Lett.* **2005**, *95*, 227401.
(9) Decker, M.; Klein, M. W.; Wegener, M.; Linden, S. Circular Dichroism of Planar Chiral Magnetic Metamaterials. *Opt. Lett.* **2007**, *32*, 856−858.
(10) Valev, V. K.; Smisdom, N.; Silhanek, a V; De Clercq, B.; Gillijns, W.; Ameloot, M.; Moshchalkov, V. V.; Verbiest, T. Plasmonic Ratchet Wheels: Switching Circular Dichroism by Arranging Chiral Nanostructures. *Nano Lett.* **2009**, *9*, 3945−3948.
(11) Hendry, E.; Mikhaylovskiy, R. V.; Barron, L. D.; Kadodwala, M.; Davis, T. J. Chiral Electromagnetic Fields Generated by Arrays of Nanoslits. *Nano Lett.* **2012**, *12*, 3640−3644.
(12) Gansel, J. K.; Thiel, M.; Rill, M. S.; Decker, M.; Bade, K.; Saile, V.; von Freymann, G.; Linden, S.; Wegener, M. Gold Helix Photonic Metamaterial as Broadband Circular Polarizer. *Science* **2009**, *325*, 1513−1515.
(13) Radke, A.; Gissibl, T.; Klotzbücher, T.; Braun, P. V.; Giessen, H. Three-Dimensional Bichiral Plasmonic Crystals Fabricated by Direct Laser Writing and Electroless Silver Plating. *Adv. Mater.* **2011**, *23*, 3018−3021.
(14) Rockstuhl, C.; Menzel, C.; Paul, T.; Lederer, F. Optical Activity in Chiral Media Composed of Three-Dimensional Metallic Meta-Atoms. *Phys. Rev. B: Condens. Matter Mater. Phys.* **2009**, *79*, 035321.
(15) Zhang, S.; Zhou, J.; Park, Y.-S.; Rho, J.; Singh, R.; Nam, S.; Azad, A. K.; Chen, H.-T.; Yin, X.; Taylor, A. J.; Zhang, X. Photoinduced Handedness Switching in Terahertz Chiral Metamolecules. *Nat. Commun.* **2012**, *3*, 942.
(16) Schäferling, M.; Yin, X.; Engheta, N.; Giessen, H. Helical Plasmonic Nanostructures as Prototypical Chiral Near-Field Sources. *ACS Photonics* **2014**, *1*, 53010.1021/ph5000743
(17) Frank, B.; Yin, X.; Schäferling, M.; Zhao, J.; Hein, S. M.; Braun, P. V.; Giessen, H. Large-Area 3D Chiral Plasmonic Structures. *ACS Nano* **2013**, *7*, 6321.
(18) Mark, A. G.; Gibbs, J. G.; Lee, T.-C.; Fischer, P. Hybrid Nanocolloids with Programmed Three-Dimensional Shape and Material Composition. *Nat. Mater.* **2013**, *12*, 1−6.
(19) Fan, Z.; Govorov, A. O. Chiral Nanocrystals: Plasmonic Spectra and Circular Dichroism. *Nano Lett.* **2012**, *12*, 3283−3289.
(20) McPeak, K. M.; van Engers, C. D.; Blome, M.; Park, J. H.; Burger, S.; Gosálvez, M. A.; Faridi, A.; Ries, Y. R.; Sahu, A.; Norris, D. J. Complex Chiral Colloids and Surfaces via High-Index off-Cut Silicon. *Nano Lett.* **2014**, *14*, 2934−2940.
(21) Dietrich, K.; Menzel, C.; Lehr, D.; Puffky, O.; Hübner, U.; Pertsch, T.; Tünnermann, A.; Kley, E.-B. Elevating Optical Activity: Efficient on-Edge Lithography of Three-Dimensional Starfish Metamaterial. *Appl. Phys. Lett.* **2014**, *104*, 193107.
(22) Guerrero-Martínez, A.; Alonso-Gómez, J. L.; Auguié, B.; Cid, M. M.; Liz-Marzán, L. M. From Individual to Collective Chirality in Metal Nanoparticles. *Nano Today* **2011**, *6*, 381.
(23) Shemer, G.; Krichevski, O.; Markovich, G.; Molotsky, T.; Lubitz, I.; Kotlyar, A. B. Chirality of Silver Nanoparticles Synthesized on DNA. *J. Am. Chem. Soc.* **2006**, *128*, 11006−11007.
(24) Zhao, Y.; Belkin, M. A.; Alù, A. Twisted Optical Metamaterials for Planarized Ultrathin Broadband Circular Polarizers. *Nat. Commun.* **2012**, *3*, 870.
(25) Christofi, A.; Stefanou, N.; Gantzounis, G.; Papanikolaou, N. Giant Optical Activity of Helical Architectures of Plasmonic Nanorods. *J. Phys. Chem. C* **2012**, *116*, 16674−16679.
(26) Liu, N.; Liu, H.; Zhu, S.; Giessen, H. Stereometamaterials. *Nat. Photonics* **2009**, *3*, 157−162.
(27) Kuzyk, A.; Schreiber, R.; Fan, Z.; Pardatscher, G.; Roller, E.-M.; Högele, A.; Simmel, F. C.; Govorov, A. O.; Liedl, T. DNA-Based Self-Assembly of Chiral Plasmonic Nanostructures with Tailored Optical Response. *Nature* **2012**, *483*, 311−314.
(28) Schreiber, R.; Luong, N.; Fan, Z.; Kuzyk, A.; Nickels, P. C.; Zhang, T.; Smith, D. M.; Yurke, B.; Kuang, W.; Govorov, A. O.; Liedl, T. Chiral Plasmonic DNA Nanostructures with Switchable Circular Dichroism. *Nat. Commun.* **2013**, *4*, 1−6.
(29) Ma, W.; Kuang, H.; Wang, L.; Xu, L.; Chang, W.-S.; Zhang, H.; Sun, M.; Zhu, Y.; Zhao, Y.; Liu, L.; Xu, C.; Link, S.; Kotov, N. A. Chiral Plasmonics of Self-Assembled Nanorod Dimers. *Sci. Rep.* **2013**, *3*, 1934.
(30) Ogier, R.; Fang, Y.; Svedendahl, M.; Johansson, P.; Käll, M. Macroscopic Layers of Chiral Plasmonic Nanoparticle Oligomers from Colloidal Lithography. *ACS Photonics* **2014**, *1*, 107410.1021/ph500293u.
(31) Fan, Z.; Govorov, A. O. Plasmonic Circular Dichroism of Chiral Metal Nanoparticle Assemblies. *Nano Lett.* **2010**, *10*, 2580−2587.
(32) Menzel, C.; Helgert, C.; Rockstuhl, C.; Kley, E.-B.; Tünnermann, A.; Pertsch, T.; Lederer, F. Asymmetric Transmission of Linearly Polarized Light at Optical Metamaterials. *Phys. Rev. Lett.* **2010**, *104*, 253902.
(33) Kenanakis, G.; Xomalis, A.; Selimis, A.; Vamvakaki, M.; Farsari, M.; Kafesaki, M.; Soukoulis, C. M.; Economou, E. N. A Three-Dimensional Infra-Red Metamaterial with Asymmetric Transmission. *ACS Photonics* **2015**, *2*, 28710.1021/ph5003818.
(34) Hendry, E.; Carpy, T.; Johnston, J.; Popland, M.; Mikhaylovskiy, R. V.; Lapthorn, A. J.; Kelly, S. M.; Barron, L. D.; Gadegaard, N.; Kadodwala, M. Ultrasensitive Detection and Characterization of Biomolecules Using Superchiral Fields. *Nat. Nanotechnol.* **2010**, *5*, 783−787.
(35) Govorov, A. O.; Fan, Z.; Hernandez, P.; Slocik, J. M.; Naik, R. R. Theory of Circular Dichroism of Nanomaterials Comprising Chiral Molecules and Nanocrystals: Plasmon Enhancement, Dipole Interactions, and Dielectric Effects. *Nano Lett.* **2010**, *10*, 1374−1382.
(36) Ren, M.; Plum, E.; Xu, J.; Zheludev, N. I. Giant Nonlinear Optical Activity in a Plasmonic Metamaterial. *Nat. Commun.* **2012**, *3*, 833.
(37) Sönnichsen, C.; Reinhard, B. M.; Liphardt, J.; Alivisatos, A. P. A Molecular Ruler Based on Plasmon Coupling of Single Gold and Silver Nanoparticles. *Nat. Biotechnol.* **2005**, *23*, 741−745.
(38) Davis, T. J.; Hentschel, M.; Liu, N.; Giessen, H. Analytical Model of the Three-Dimensional Plasmonic Ruler. *ACS Nano* **2012**, *6*, 1291−1298.
(39) Ferry, V. E.; Smith, J. M.; Alivisatos, A. P. Symmetry Breaking in Tetrahedral Chiral Plasmonic Nanoparticle Assemblies. *ACS Photonics* **2014**, *1*, 1189.
(40) Hentschel, M.; Schäferling, M.; Weiss, T.; Liu, N.; Giessen, H. Three-Dimensional Chiral Plasmonic Oligomers. *Nano Lett.* **2012**, *12*, 2542−2547.
(41) Halas, N. J.; Lal, S.; Chang, W.-S.; Link, S.; Nordlander, P. Plasmons in Strongly Coupled Metallic Nanostructures. *Chem. Rev.* **2011**, *111*, 3913−3961.

DOI: 10.1021/acsphotonics.5b00354
ACS Photonics 2015, 2, 1253−1259

(42) Valev, V. K.; Baumberg, J. J.; Sibilia, C.; Verbiest, T. Chirality and Chiroptical Effects in Plasmonic Nanostructures: Fundamentals, Recent Progress, and Outlook. *Adv. Mater.* **2013**, *25*, 2517−2534.
(43) Decker, M.; Zhao, R.; Soukoulis, C. M.; Linden, S.; Wegener, M. Twisted Split-Ring-Resonator Photonic Metamaterial with Huge Optical Activity. *Opt. Lett.* **2010**, *35*, 1593−1595.
(44) Yin, X.; Schäferling, M.; Metzger, B.; Giessen, H. Interpreting Chiral Nanophotonic Spectra: The Plasmonic Born-Kuhn Model. *Nano Lett.* **2013**, *13*, 6238−6243.
(45) Johnson, P. B.; Christy, R. W. Optical Constants of the Noble Metals. *Phys. Rev. B* **1972**, *6*, 4370−4379.

DOI: 10.1021/acsphotonics.5b00354
ACS Photonics 2015, 2, 1253−1259